Table 4. Results of the Multiple Regression Analyses for the GDx VCC Parameters Associated with the Corresponding Visual Filed Damage

Parameter	n-AION		OAG	
	Standardized β	*P Value*	*Standardized β*	*P Value*
TSNIT average for MD	0.41	0.045	0.42	0.022
Inferior average for TD_{sup}	0.67	<0.001	0.31	0.102
Superior average for TD_{inf}	0.59	0.003	0.38	0.039

GDx VCC = GDx Nerve Fiber Analyzer with Variable Corneal Compensation; MD = mean deviation; n-AION = nonarteritic anterior ischemic optic neuropathy; OAG = open-angle glaucoma; TSNIT average = ellipse average; TD_{sup} = average of total deviation in the superior hemifield; TD_{inf} = average of total deviation in the inferior hemifield.

The current study is also the first documentation of RNFL thickness measured using SLP with VCC in eyes after n-AION. Banks et al[13] measured the RNFL thickness in eyes with n-AION or AION using SLP with FCC.[13] Those authors reported the average thicknesses as 59±7 and 51±9 μm in the acute (n = 18 eyes) and chronic (n = 20 eyes) phases, respectively. Colen et al.[14] reported the follow-up of 1 case of n-AION using SLP with FCC, in which the RNFL thickness (the "superior average") decreased from 62 μm 10 days after onset to 48 μm 9 months later. Compared to those reports, the TSNIT averages in 33 n-AION eyes of the current study (40.7±11.0 μm) were relatively smaller. Because anterior segment birefringence varies widely in human eyes, SLP with FCC often provides inappropriate data on RNFL thickness.[17,18] Moreover, the RNFL thickness values tend to be higher with FCC than with VCC,[18] possibly explaining the discrepancy in RNFL thickness in n-AION eyes between the current and previous studies.[13,14]

In the n-AION eyes of this study, the superior average of RNFL thickness was significantly smaller than the inferior average. This is contrary to the results in normal[19,20] or OAG[19] eyes and the current results on OAG, and suggested that the superior region of the ONH was more commonly affected in n-AION. Although the HRT parameters did not significantly correlate with VFD, the results of GDx VCC were significantly associated with the corresponding VFD with regression coefficients of 0.41 to 0.67 (Table 3).

Eyes with slight cataract were included in the current study. Even slight cataract can possibly affect the results of visual field testing. However, Carrillo et al[21] recently reported that the average change in MD after extraction of cataract in OAG patients whose preoperative log MAR visual acuity averaged 0.24 (between 20/30 and 20/40) was <0.1 dB and not statistically significant, suggesting that at least slight or mild cataract should not have apparent effects on the average of MD in a group of patients. Moreover, in the current study, because age of the n-AION patients and that of the OAG patients were matched (61.8±10.4 vs. 61.8±10.3 years), the total amount of the influence of (slight) cataract should be similar between the 2 groups, if it existed.

Most of the patients with n-AION had no experience with visual field testing using the HFA prior to this study, whereas the patients with OAG had several experiences. According to Heijl et al,[22] improvement of MD between the initial and second tests of the HFA in newly diagnosed glaucoma patients averaged 2.81 dB, which corresponded to 23% of the average of MD of the current n-AION eyes (−12.3 dB). Therefore, differences in the HRT parameters between the n-AION eyes and the OAG eyes, which ranged 30% to 320% (Table 2), cannot be explained completely by the influence of learning effects in the HFA testing.

In conclusion, the ONH topography in n-AION eyes was quantitatively characterized by small and shallow cupping and a relatively larger rim area compared to the age- and MD-matched OAG eyes. In n-AION eyes, the RNFL thickness evaluated with GDx VCC showed a good correlation with VFD, whereas the HRT results did not significantly correlate with VFD.

References

1. Hayreh SS. Anterior ischaemic optic neuropathy. II. Fundus on ophthalmoscopy and fluorescein angiography. Br J Ophthalmol 1974;58:964–80.
2. Tesser RA, Niendorf ER, Levin LA. The morphology of an infarct in nonarteritic anterior ischemic optic neuropathy. Ophthalmology 2003;110:2031–5.
3. Salomon O, Huna-Baron R, Kurtz S, et al. Analysis of prothrombotic and vascular risk factors in patients with nonarteritic anterior ischemic optic neuropathy. Ophthalmology 1999;106:739–42.
4. Repka MX, Savino PJ, Schatz NJ, Sergott RC. Clinical profile and long-term implications of anterior ischemic optic neuropathy. Am J Ophthalmol 1983;96:478–83.
5. Jacobson DM, Vierkant RA, Belongia EA. Nonarteritic anterior ischemic optic neuropathy. A case-control study of potential risk factors. Arch Ophthalmol 1997;115:1403–7.
6. Landau K, Winterkorn JM, Mailloux LU, et al. 24-hour blood pressure monitoring in patients with anterior ischemic optic neuropathy. Arch Ophthalmol 1996;114:570–5.
7. Hayreh SS, Zimmerman MB, Podhajsky P, Alward WL. Nonarteritic anterior ischemic optic neuropathy: role of nocturnal arterial hypotension. Arch Ophthalmol 1997;115:942–5.
8. Burde RM. Optic disk risk factors for nonarteritic anterior ischemic optic neuropathy. Am J Ophthalmol 1993;116:759–64.
9. Mansour AM, Shoch D, Logani S. Optic disk size in ischemic optic neuropathy. Am J Ophthalmol 1988;106:587–9.
10. Jonas JB, Xu L. Optic disc morphology in eyes after nonarteritic anterior ischemic optic neuropathy. Invest Ophthalmol Vis Sci 1993;34:2260–5.

11. Doro S, Lessell S. Cup-disc ratio and ischemic optic neuropathy. Arch Ophthalmol 1985;103:1143–4.
12. Beck RW, Servais GE, Hayreh SS. Anterior ischemic optic neuropathy. IX. Cup-to-disc ratio and its role in pathogenesis. Ophthalmology 1987;94:1503–8.
13. Banks MC, Robe-Collignon NJ, Rizzo JF III, Pasquale LR. Scanning laser polarimetry of edematous and atrophic optic nerve heads. Arch Ophthalmol 2003;121:484–90.
14. Colen TP, van Everdingen JA, Lemij HG. Axonal loss in a patient with anterior ischemic optic neuropathy as measured with scanning laser polarimetry. Am J Ophthalmol 2000;130: 847–50.
15. Danesh-Meyer H, Savino PJ, Spaeth GL, Gamble GD. Comparison of arteritis and nonarteritic anterior ischemic optic neuropathies with the Heidelberg Retina Tomograph. Ophthalmology 2005;112:1104–12.
16. Quigley H, Anderson DR. Cupping of the optic disc in ischemic optic neuropathy. Trans Sect Ophthalmol Am Acad Ophthalmol Otolaryngol 1977;83:755–62.
17. Weinreb RN, Bowd C, Greenfield DS, Zangwill LM. Measurement of the magnitude and axis of corneal polarization with scanning laser polarimetry. Arch Ophthalmol 2002;120:901–6.
18. Zhou Q, Weinreb RN. Individualized compensation of anterior segment birefringence during scanning laser polarimetry. Invest Ophthalmol Vis Sci 2002;43:2221–8.
19. Medeiros FA, Zangwill LM, Bowd C, Weinreb RN. Comparison of the GDx VCC scanning laser polarimeter, HRT II confocal scanning laser ophthalmoscope, and Stratus OCT optical coherence tomograph for the detection of glaucoma. Arch Ophthalmol 2004;122:827–37.
20. Kremmer S, Zadow T, Steuhl KP, Selbach JM. Scanning laser polarimetry in myopic and hyperopic subjects. Graefes Arch Clin Exp Ophthalmol 2004;242:489–94.
21. Carrillo MM, Artes PH, Nicolela MT, et al. Effect of cataract extraction on the visual fields of patients with glaucoma. Arch Ophthalmol 2005;123:929–32.
22. Heijl A, Bengtsson B. The effect of perimetric experience in patients with glaucoma. Arch Ophthalmol 1996;114:19–22.

Eye (2006), 1–6

www.nature.com/eye

CLINICAL STUDY

Performance of GDx VCC in eyes with peripapillary atrophy: comparison of three circle sizes

S Kunimatsu, A Tomidokoro, H Saito, M Aihara, G Tomita and M Araie

Abstract

Purpose A scanning laser polarimetry (GDx VCC) equips three different sized measurement circles. In eyes with peripapillary atrophy (PPA), the GDx measurement becomes inaccurate when the circle falls on PPA. The aim of this study was to evaluate performance of the three circles of GDx measurement in eyes with PPA.

Methods Three different sized circles were compared regarding frequency of PPA, which fell on each circle in 282 open-angle glaucoma (OAG) eyes, reproducibility of GDx parameters in 24 normal and 22 OAG eyes, and ability to detect glaucoma in 50 normal and 50 OAG eyes.

Results PPA was observed in 230 (82%) of 282 OAG eyes. PPA fell on the small circle (default setting), medium, and large circles in 119 (43%), 38 (14%), and 12 (4%) of the 280 OAG eyes. Reproducibility of GDx parameters was not significantly different among three circles in normal eyes ($P>0.05$), whereas coefficients of reproducibility of TSNIT average ($P=0.006$) and superior average ($P=0.035$) were smaller in the smaller circles in OAG eyes. GDx parameters significantly correlated ($P<0.001$), but were significantly different ($P<0.05$) between the small and medium circles. The area under receiver operating characteristic curves for dividing OAG from normal eyes using GDx parameters was similar between the small and medium circles.

Conclusions If the medium circles were used, obstructing influences of PPA on GDx measurement could be avoided more often in Japanese OAG eyes with similar reproducibility and comparable ability to detect glaucoma compared to those with the default small circle.

Eye advance online publication, 4 August 2006; doi:10.1038/sj.eye.6702516

Keywords: peripapillary atrophy; GDx; VCC; open-angle glaucoma; scanning laser polarimetry

Introduction

Accuracy of measurements of the retinal nerve fiber layer (RNFL) thickness using a scanning laser polarimetry (SLP), GDx (Carl Zeiss Meditec, Dublin, CA, USA), has been improved after the introduction of the variable corneal compensation (VCC) system, which reduces the influence of the anterior segment birefringence in an individual eye.[1–4] However, one of the remaining drawbacks of SLP is that RNFL measurements are inaccurate when peripapillary atrophy (PPA) fell on the measurement circle (Figure 1). As PPA is more frequent in myopic eyes[5,6] and myopia is much more common among Japanese,[7] it is supposed that PPA is commonly accompanied with Japanese patients of open-angle glaucoma (OAG).

With new software (GDx VCC version 5.3.2.), two different sizes of circles (medium and large) are available in addition to the default size circle (small). The inner diameters are 2.4, 3.2, and 4.0 mm for small, medium, and large circles, respectively, in eyes with normal refraction, although the actual sizes will be altered according to the refractive error of each eye. Using the medium or large circle instead of the default small circle, the obstructing influence of PPA on the RNFL measurement would be often avoided. To our knowledge, however, no report is available on the clinical usefulness of the medium or large circle. The aim of this study was to estimate the frequency of PPA in Japanese OAG eyes and to assess the reliability and usefulness of the RNFL measurements

Department of Ophthalmology, University of Tokyo Graduate School of Medicine, Tokyo, Japan

Correspondence:
A Tomidokoro,
Department of Ophthalmology, University of Tokyo Graduate School of Medicine,
7-3-1 Hongo, Bunkyo-ku, Tokyo 113-8655, Japan
Tel: +81 3 3815 5411;
Fax: +81 3 3897 0798.
E-mail: tomidokoro-tky@umin.ac.jp

Received: 26 January 2006
Accepted: 12 June 2006

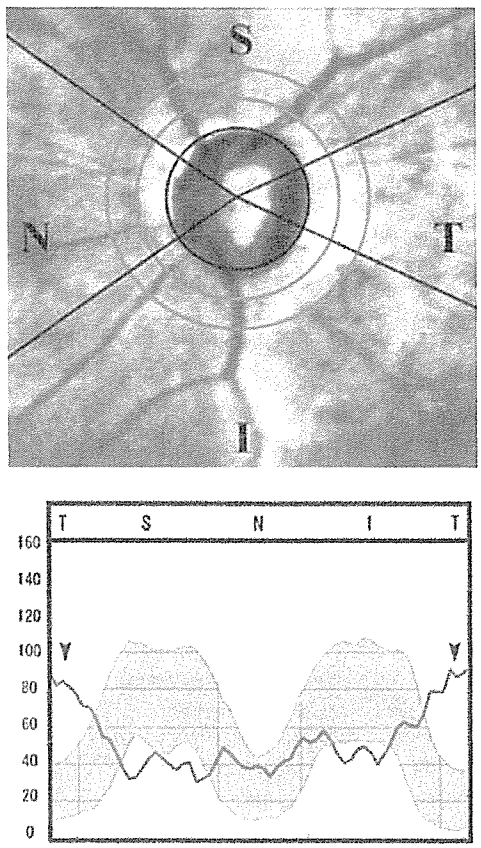

Figure 1 An example of GDx VCC measurements in eyes with PPA. This eye has a large PPA and the temporal portion of the PPA falls on the measurement circle (small circle) (a). As the consequence, retinal neve fiber layer thickness is measured abnormally thicker in the temporal area (arrowheads, b).

using medium or large circle for those eyes in which the small circle would fall on the area with PPA.

Methods

The studies below were carried out at the Department of Ophthalmology of the University of Tokyo, Graduate School of Medicine. Written informed consent to use their clinical data for this study was obtained from all subjects. The study was approved by the Institutional Review Board for Human Research of the University of Tokyo, Graduate School of Medicine and was conducted according to the tenets of the Declaration of Helsinki.

Measurement of GDx VCC

SLP images were obtained using GDx VCC with a software version 5.3.2. The general principles of SLP have been described in detail elsewhere.[8,9] Imaging was obtained under dim light and with undilated pupils. For each eye, the macula was imaged without compensation, and the eye-specific corneal polarization axis and corneal polarization magnitude were recorded. Corneal birefringence-compensated SLP images then were acquired using the eye-specific corneal polarization axis and magnitude by adjusting the VCC retarder. Determination of the GDx VCC parameters was performed with regard to the small (default), medium, and large circles, respectively, on each acquired image with quality score of 8 or more.

Frequency of PPA falling on circles in OAG eyes

The frequency of eyes in which PPA fell on each of the GDx circles was determined using the stocked data of 282 eyes of 141 OAG patients continuously obtained between September 2003 and May 2004. A diagnosis of OAG was made according to the typical glaucomatous optic disc findings, the corresponding visual field damage, and the absence of any contributing ocular or systemic disorders in disregard of intraocular pressure (IOP). Eyes with refractive errors (spherical equivalent) larger than 8 D and eyes had history of intraocular surgery including laser were not included. The patients studied included 81 male and 60 female patients and age averaged 55.4±12.3 (mean±SD) years, refractive error −3.9±3.5 D, IOP with or without medication 18.3±3.9 mmHg, and mean deviation (MD) of the Humphrey Field Analyzer 30-2 SITA standard (Carl Zeiss Meditec, Dublin, CA, USA) −6.0±5.4 dB.

The GDx VCC results of each patient were reloaded from the hard disc drive of the instrument and the small, medium, and large circles were drawn. Beta zone of PPA, which was identified by choroidal atrophy with visible large choroidal vessels and sclera, was determined and judged whether each of the measurement circles fell on the PPA or not on the display of GDx VCC instrument with the help of colour fundus photographs if necessary. Alpha zone of PPA, which located peripherally and characterized by irregular hypopigmentation, hyperpigmentation, or both, was not included in the current study.

Reproducibility of the GDx measurements using the three circles

Reproducibility of GDx VCC parameters obtained with three circles was evaluated in 24 eyes of 16 ophthalmologically healthy subjects (mean age, 35.1±6.2 years) and 22 eyes of 14 patients with OAG (mean age, 53.8±13.6 years) in whom the data were newly obtained. The criteria of the diagnosis of OAG were same as above. In the OAG patients, refractive error averaged −3.3±3.7 D, IOP with or without medication 14.1±3.1 mmHg, and MD −5.6±5.5 dB.

Ophthalmologically healthy subjects had IOP not exceeding 21 mmHg, the optic disc with a normal appearance, a normal open angle, a normal visual field defined, and had no history of ocular diseases or a family history of glaucoma. In the ophthalmologically healthy subjects, refractive error averaged -1.0 ± 1.4 D.

Each eye was scanned twice on separate days within a 1-month period. Eyes were excluded when any of the three circles fell on PPA or image quality fell below 8. The coefficient of the reproducibility for each parameter was calculated as follows: $|V_1\text{-}V_2|/(V_1+V_2)/2 \times 100\%$, where V_1 is the first and V_2 the second measurement obtained.

Mean values of the GDx parameters and detection of glaucoma

As the fraction of poor-quality images is rather high for the large circle (see Results section), the performance of the GDx was not determined for this circle size. Comparison of the GDx parameters between 50 ophthalmologically normal eyes of 50 subjects (mean age, 50.6 ± 8.7 years) and 50 OAG eyes of 50 patients (mean age, 49.4 ± 9.1 years), of whom data were newly obtained for this part of the current study, and ability to detect glaucomatous eyes using GDx VCC was evaluated. The criteria of ophthalmologically healthy subjects and the diagnosis of OAG patients were same as above. In the OAG patients, refractive error averaged -3.6 ± 2.5 D, IOP with or without medication 14.2 ± 3.3 mmHg, and MD -4.2 ± 2.9 dB. In the ophthalmologically healthy subjects, refractive error averaged -0.8 ± 1.6 D.

Statistical analysis

Statistical analyses were performed using a statistical software package, SPSS 13.0J for Windows (SPSS Japan Inc., Tokyo, Japan). Friedman's test was used to compare the averages among three groups. The difference between two groups was evaluated using the Wilcoxon's signed-rank test or the χ^2 test. Statistical correlation was evaluated by Spearman's rank correlation coefficient.

Receiver operating characteristic (ROC) curves were used to describe the ability to differentiate OAG eyes from normal eyes. A P-value less than 0.05 was considered statistically significant.

Results

Frequency of PPA falling on circles in OAG eyes

PPA could not be determined owing to expanded chorioretinal atrophy around the optic disc in two eyes. PPA was observed in 230 (82%) of the remaining 280 OAG eyes. PPA fell on the small, medium, and large circles in 119 (43%), 38 (14%), and 12 (4%) of the 280 eyes, respectively. The frequency with small circle was significantly greater than that with medium circle ($P<0.001$), and that with medium circle was greater than that with large circle ($P<0.001$). The GDx VCC

Table 1 Coefficient of reproducibility for the GDx parameters obtained with small, medium, and large circles in normal and OAG eyes

	Small circle	*Medium circle*	*Large circle*	*P-values**
TSNIT average				
Normal	3.3 (1.6, 5.1)	4.3 (1.9, 6.6)	5.0 (2.1, 8.0)	0.14
OAG	4.5 (0.7, 8.3)	6.2 (1.1, 11.2)	7.8 (2.8, 12.9)	0.006
Superior average				
Normal	3.7 (2.3, 5.1)	4.6 (2.5, 6.7)	5.2 (2.5, 7.9)	0.5
OAG	2.2 (0.7, 3.8)	3.1 (0.2, 6.0)	4.6 (1.1, 8.1)	0.035
Inferior average				
Normal	4.6 (2.5, 6.6)	4.8 (2.3, 7.3)	5.7 (2.9, 8.6)	0.080
OAG	7.5 (2.6, 12.4)	14.2 (1.5, 27.0)	14.9 (5.5, 24.2)	0.078
TSNIT SD				
Normal	7.4 (4.4, 10.4)	7.2 (4.3, 10.0)	7.0 (4.1, 9.9)	0.9
OAG	8.2 (4.1, 12.3)	7.4 (3.6, 11.1)	10.7 (5.8, 15.6)	0.060
NFI				
Normal	13.3 (8.2, 20.3)	19.5 (13.4, 29.2)	20.8 (10.9, 29.1)	0.054
OAG	17.6 (9.0, 26.2)	19.4 (7.8, 30.9)	16.7 (5.9, 27.5)	0.6

NFI, nerve fiber indicator; OAG, open-angle glaucoma; SD, standard deviation.
Data are shown with 95% confidence interval in the parentheses.
*P-value for difference among three circles (Friedman's test).

parameters could not be obtained in 34 (12%), 41 (15%), and 71 (25%) of 282 eyes for the small, medium, and large circles, respectively, because of poor image quality score (<8) or extrusion of the circle from the measurement area. Those frequencies were significantly different among the circles ($P<0.001$, χ^2 test) and the frequency with the large circle was significantly larger than that with the small or medium circle ($P<0.001$, $P=0.002$, respectively).

Reproducibility of the measurements using the three circles

Coefficients of reproducibility of the GDx parameters in normal or OAG eyes are shown in Table 1. These were not significantly different among the three circles in normal eyes for each parameter ($P>0.05$, Friedman's test), whereas coefficients of reproducibility of TSNIT average ($P=0.006$) and superior average ($P=0.035$) were smaller in the smaller circles in OAG eyes.

Mean values of the GDx parameters and detection of glaucoma

Mean values of the GDx parameters are shown in Table 2. All parameters in OAG eyes were significantly smaller than in normal eyes ($P<0.05$, Wilcoxon's signed-rank test). Between the small and medium circles, all of the GDx parameters significantly correlated (Spearman's rank correlation coefficients >0.8, $P<0.001$).

The ROC curves for dividing OAG eyes from normal eyes using each parameter obtained with the small and medium circles were determined. The area under the ROC curves is shown in Table 3. Ninety-five percent confidence interval was overlapping each other between the small and medium circles, suggesting there was no apparent difference in the ability to detect OAG eyes between these circles. Among the indices, the nerve fiber indicator (NFI) had the largest area under the ROC curve. ROC curves regarding TSNIT average and NFI are drawn in Figure 2.

Table 3 Area under the ROC for dividing glaucomatous from normal eyes using the small and medium circles

	Small circle	*Medium circle*
TSNIT average	0.90 (0.85, 0.96)	0.83 (0.74, 0.91)
Superior average	0.86 (0.78, 0.93)	0.86 (0.78, 0.93)
Inferior average	0.91 (0.86, 0.97)	0.85 (0.78, 0.92)
TINIT SD	0.80 (0.71, 0.88)	0.84 (0.76, 0.91)
NFI	0.94 (0.90, 0.99)	0.93 (0.88, 0.98)

NFI, nerve fiber indicator; ROC, receiver operating curve; SD, standard deviation.
Data (area under the ROC) are shown with 95% confidence interval in the parentheses.

Table 2 Differences and correlation of the GDx parameters between normal and OAG eyes

	Small circle		*Medium circle*		*Small vs medium circles*	
	Mean (95% CI)	*P-values*[a]	*Mean (95% CI)*	*P-values*[a]	*Correlation (P-value)*	*P-values*[b]
TSNIT average						
Normal	56 (54, 57)	<0.001	49 (48, 51)	<0.001	0.89 (<0.001)	<0.001
OAG	46 (44, 48)		42 (40, 43)		0.86 (<0.001)	<0.001
Superior average						
Normal	68 (67, 70)	<0.001	59 (58, 61)	<0.001	0.89 (<0.001)	<0.001
OAG	55 (52, 59)		48 (45, 50)		0.93 (<0.001)	<0.001
Inferior average						
Normal	66 (63, 68)	<0.001	59 (57, 61)	<0.001	0.94 (<0.001)	<0.001
OAG	49 (46, 53)		47 (44, 50)		0.85 (<0.001)	<0.001
TSNIT SD						
Normal	23 (22, 24)	<0.001	21 (20, 23)	<0.001	0.96 (<0.001)	<0.001
OAG	19 (16, 22)		16 (15, 17)		0.90 (<0.001)	<0.001
NFI						
Normal	18 (16, 20)	<0.001	17 (15, 18)	<0.001	0.82 (<0.001)	0.027
OAG	44 (39, 49)		42 (37, 47)		0.82 (<0.001)	0.008

CI, confidence interval; NFI, nerve fiber indicator; SD, standard deviation.
Data are shown with 95% confidence interval (95% CI) in the parentheses.
[a]*P*-value for the difference of the means between normal and OAG eyes (Mann–Whitney *U*-test). Correlation = Spearman's rank correlation coefficient (with *P*-value) between small and medium circles.
[b]*P*-value for the difference of means between small and medium circles (Wilcoxon's signed-rank test).

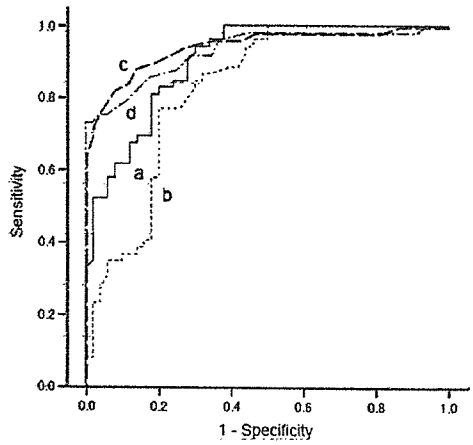

Figure 2 The ROC curves for discriminating between normal and glaucomatous eyes regarding TSNIT average of the small circle (a), that of the medium circle (b), the NFI of the small circle (c), and that of the medium circle (d).

Discussion

Frequency of PPA falling on circles on OAG eyes

The presence of PPA reduces the accuracy of the RNFL measurement using a SLP. Bowd *et al*[4] reported that in five of 73 (7%) eyes the circle fell on PPA and they used the expanded circle (20% horizontally and 20% vertically) for the analysis of those eyes. PPA is more frequently and more extensively observed in patients with glaucoma than in normal subjects in Caucasians[10,11] (no data available in Japanese) and associated with glaucomatous damage.[12–14] Because myopia is more likely associated with PPA,[5,6] and more frequent in Japan,[7] the influence of PPA on the measurement of the RNFL is of practical concern, especially in Japanese patients with OAG. In the current study, PPA fell on the small circle (default setting) in 119 (43%) of 280 OAG eyes, suggesting that accurate GDx measurement may be often disturbed because of PPA in Japanese OAG eyes when using the small circle.

When using optical coherence tomography (OCT), Lai *et al*[15] reported good agreement between the automated and manual tracing results in eyes with PPA, and the authors concluded that automated optic nerve head analysis using OCT may be used in the clinical setting in eyes with PPA. In contrast, the accuracy of GDx VCC when measuring the RNFL thickness decreases in the presence of PPA (Figure 1), and alternative measurement methods should have clinical value.

In the current study, the GDx parameters for the small, medium, and large circles could not be obtained in 34 (12%), 41 (15%), and 71 (25%) of 282 OAG eyes, respectively, because of poor image quality score (<8) or deviancy of the circle from the measurement area. Unless the optic disc was successfully located at the centre of the measurement area, the large circle easily extrude from the area. Moreover, the measurement using the large circle should be unstable because of the influence of the thinner RNFL, which was reported to often show atypical retardation pattern (ARP).[16–18]

Reproducibility of the measurements using the three circles

Good intraoperator and interoperator measurement reproducibility using an SLP has been reported by several investigators.[19–21] In the present study, we evaluated the difference in intraoperator reproducibility among the circles (Table 1). The coefficients of reproducibility in normal eyes were 8% or less, except NFI, and there was no significant difference among the three different sized circles. On the other hand, in the glaucomatous eyes, the reproducibility of some parameters was worse for the larger circles than the small ones. The sensitivity of GDx VCC is reported to be reduced in the retinal area with ARP.[16–18] This should be at least partially responsible for the poor reproducibility of the measurements with the outer circles. And besides, the influence of ARP owing to the outer and thinner retinal area should be involved with the performance in diagnosing glaucoma or assessing glaucoma progression described below.

Mean values of the GDx parameters and detection of glaucoma

Varma *et al*[22] measured histologically the thickness of the RNFL in normal human eyes and reported that the thickness decreased with increasing distance from the disc margin. In this study, the RNFL thickness obtained with the small circle was greater than that with the medium circle in normal and glaucomatous eyes, which is consistent with histologic results.

To determine the ability of each parameter to differentiate glaucomatous from normal eyes, we analysed the ROC curves. The largest area under the curve (AUC) was the NFI (0.94 with the small circle, 0.93 with the medium circle), which was similar to a previous study. Medeiros *et al*[23] reported that the AUC for NFI using GDx VCC was 0.91. There was no apparent difference between the small and medium circles when differentiating glaucoma from normal eyes. In the present version of GDx VCC, the NFI has been trained on data measured along the small circle. If a newly trained NFI, which is specially designed for the medium circle, is available, performance to detect glaucoma using the medium circle would be improved. Moreover, the

potential for the assessment of glaucoma progression may differ among the different circle sizes.

Not only beta zone of PPA but also alpha zone often shows ARP and can assert influence on GDx VCC measurements. However, because the precise determination of alpha area was difficult in some of the eyes as reported previously,[14] alpha area was not included in the present analyses. Therefore, in the current study, even if the larger circles were used and beta zone was not involved in the SLP measurement area, the disturbance of alpha zone of PPA might be still remained. Recently, a new software version, named the enhanced corneal compensation (ECC), was published.[16–18] It is reported to significantly diminish the artefacts owing to ARP. This new software may improve the performance of GDx in eyes with PPA even when using the small circle. However, whether the influence of PPA can be completely diminished with ECC is still unclear and further investigation on ECC measurements using the different measurement circles should deserve future investigation.

In conclusion, measurements with the medium circle may be a useful alternative, especially in Japan[7] and other East-Asian countries where the prevalence of myopia with PPA is higher than in Western countries.[24,25]

References

1 Weinreb RN, Bowd C, Zangwill LM. Glaucoma detection using scanning laser polarimetry with variable corneal polarization compensation. *Arch Ophthalmol* 2002; **120**: 218–224.

2 Greenfield DS, Knighton RW, Feuer WJ, Schiffman JC, Zangwill L, Weinreb RN. Correction for corneal polarization axis improves the discriminating power of scanning laser polarimetry. *Am J Ophthalmol* 2002; **134**: 27–33.

3 Bagga H, Greenfield DS, Feuer W, Knighton RW. Scanning laser polarimetry with variable corneal compensation and optical coherence tomography in normal and glaucomatous eyes. *Am J Ophthalmol* 2003; **135**: 521–529.

4 Bowd C, Zangwill LM, Weinreb RN. Association between scanning laser polarimetry measurements using variable corneal polarization compensation and visual field sensitivity in glaucomatous eyes. *Arch Ophthalmol* 2003; **121**: 961–966.

5 Ramrattan RS, Wolfs RC, Jonas JB, Hofman A, de Jong PT. Determinants of optic disc characteristics in a general population: The Rotterdam Study. *Ophthalmology* 1999; **106**: 1588–1596.

6 Vongphanit J, Mitchell P, Wang JJ. Population prevalence of tilted optic disks and the relationship of this sign to refractive error. *Am J Ophthalmol* 2002; **133**: 679–685.

7 Shiose Y, Kitazawa Y, Tsukahara S, Akamatsu T, Mizokami K, Futa R *et al*. Epidemiology of glaucoma in Japan: a nationwide glaucoma survey. *Jpn J Ophthalmol* 1991; **35**: 133–135.

8 Weinreb RN, Shakiba S, Zangwill L. Scanning laser polarimetry to measure the nerve fiber layer of normal and glaucomatous eyes. *Am J Ophthalmol* 1995; **119**: 627–636.

9 Zhou Q, Weinreb RN. Individualized compensation of anterior segment birefringence during scanning laser polarimetry. *Invest Ophthalmol Vis Sci* 2002; **43**: 2221–2228.

10 Jonas JB, Nguyen XN, Gusek GC, Naumann GO. Peripapillary chorioretinal atrophy in normal and glaucoma eyes. I. Morphometric data. *Invest Ophthalmol Vis Sci* 1989; **5**: 908–918.

11 Jonas JB, Konigsreuther KA, Naumann GO. Optic disc histomorphometry in normal eyes and eyes with secondary angle-closure glaucoma. II. Peripapillary region. *Graefe's Arch Clin Exp Ophthalmol* 1992; **230**: 134–139.

12 Jonas JB, Naumann GO. Peripapillary chorioretinal atrophy in normal and glaucoma eyes. II. Correlations. *Invest Ophthalmol Vis Sci* 1989; **30**: 919–926.

13 Jonas JB, Fernandez MC, Naumann GO. Glaucomatous peripapillary atrophy. Occurrence and correlations. *Arch Ophthalmol* 1992; **110**: 214–222.

14 Park KH, Tomita G, Liou SY, Kitazawa Y. Correlation between peripapillary atrophy and optic nerve damage in normal-tension glaucoma. *Ophthalmology* 1996; **103**: 1899–1906.

15 Lai E, Wollstein G, Price LL, Paunescu LA, Stark PC, Fujimoto JG *et al*. Optical coherence tomography disc assessment in optic nerves with peripapillary atrophy. *Ophthalmic Surg Lasers Imag* 2003; **34**: 498–504.

16 Toth M, Hollo G. Evaluation of enhanced corneal compensation in scanning laser polarimetry: comparison with variable corneal compensation on human eyes undergoing LASIK. *J Glaucoma* 2006; **15**: 53–59.

17 Toth M, Hollo G. Enhanced corneal compensation for scanning laser polarimetry on eyes with atypical polarisation pattern. *Br J Ophthalmol* 2005; **89**: 1139–1142.

18 Sehi M, Guaqueta DC, Greenfield DS. An enhancement module to improve the atypical birefringence pattern using scanning laser polarimetry with variable corneal compensation. *Br J Ophthalmol* 2006; **90**: 749–753.

19 Hoh ST, Ishikawa H, Greenfield DS, Liebmann JM, Chew SJ, Ritch R. Peripapillary nerve fiber layer thickness measurement reproducibility using scanning laser polarimetry. *J Glaucoma* 1998; **7**: 12–15.

20 Kook MS, Sung K, Park RH, Kim KR, Kim ST, Kang W. Reproducibility of scanning laser polarimetry (GDx) of peripapillary retinal nerve fiber layer thickness in normal subjects. *Graefe's Arch Clin Exp Ophthalmol* 2001; **239**: 118–121.

21 Rhee DJ, Greenfield DS, Chen PP, Schiffman J. Reproducibility of retinal nerve fiber layer thickness measurements using scanning laser polarimetry in pseudophakic eyes. *Ophthalmic Surg Lasers* 2002; **33**: 117–122.

22 Varma R, Skaf M, Barron E. Retinal nerve fiber layer thickness in normal human eyes. *Ophthalmology* 1996; **103**: 2114–2119.

23 Medeiros FA, Zangwill LM, Bowd C, Weinreb RN. Comparison of the GDx VCC scanning laser polarimeter, HRT II confocal scanning laser ophthalmoscope, and stratus OCT optical coherence tomograph for the detection of glaucoma. *Arch Ophthalmol* 2004; **122**: 827–837.

24 Mutti DO, Bullimore MA. Myopia: an epidemic of possibilities? *Optom Vis Sci* 1999; **76**: 257–258.

25 Saw SM, Katz J, Schein OD, Chew SJ, Chan TK. Epidemiology of myopia. *Epidemiol Rev* 1996; **18**: 175–187.

Correlation Between Hemifield Visual Field Damage and Corresponding Parapapillary Atrophy in Normal-Tension Glaucoma

JUNKO KAWANO, MD, ATSUO TOMIDOKORO, MD, CHIHIRO MAYAMA, MD, SHIHO KUNIMATSU, MD, GOJI TOMITA, MD, AND MAKOTO ARAIE, MD

• PURPOSE: To evaluate the correlation between the superior or inferior half area of parapapillary atrophy (PPA) and the corresponding hemifield visual field damage (VFD) in normal-tension glaucoma.

• DESIGN: Cross-sectional study.

• METHODS: PATIENTS: One hundred nine eyes of 109 consecutive patients with normal-tension glaucoma. OBSERVATION PROCEDURES: Topography parameters of the optic nerve head and PPA (zone β) area were obtained with the Heidelberg Retina Tomograph (HRT), and VFD was evaluated with the 30 to 2 program of Humphrey Field Analyzer. The HRT parameters and PPA area were determined separately in superior and inferior half regions. MAIN OUTCOME MEASURES: Partial correlation coefficients of the superior and inferior areas of PPA with refractive error, axial length, HRT parameters, and corresponding hemifield VFD.

• RESULTS: In simple correlation analyses, significant correlation was found between the inferior PPA area and the superior hemifield VFD (Spearman rank correlation coefficient; $Rs = -0.32$; $P < .001$) but not between the superior PPA area and the inferior hemifield VFD ($Rs = 0.05$; $P = .6$). Age, refractive error, axial length, and height variation contour were associated significantly with the total, superior, and inferior areas of PPA, respectively ($P < .01$). Multiple regression analyses showed that the superior PPA area was associated significantly with only axial length ($P < .001$), and the inferior PPA area was associated significantly with the axial length and the superior hemifield VFD ($P < .001$).

• CONCLUSIONS: In patients with normal-tension glaucoma, only the inferior half area of PPA correlated significantly with glaucomatous VFD. Axial length and myopia were associated with both the superior and inferior half areas of PPA. (Am J Ophthalmol 2006; 142:40–45. © 2006 by Elsevier Inc. All rights reserved.)

Accepted for publication Jan 30, 2006.

From the Department of Ophthalmology, University of Tokyo Graduate School of Medicine, Bunkyo-ku, Tokyo, Japan.

Inquiries to Atsuo Tomidokoro, MD, Department of Ophthalmology, University of Tokyo School of Medicine, 7-3-1, Hongo, Bunkyo-ku, Tokyo, 113-8655, Japan; e-mail: tomidokoro-tky@umin.ac.jp

PARAPAPILLARY ATROPHY (PPA) IS RELATED CLOSELY to the development and progression of open-angle glaucoma. PPA develops more frequently and is more extensive in eyes with glaucoma[1–3] than in eyes with ocular hypertension[4] or eyes with a so-called glaucoma-like disk,[5] compared with normal eyes; a significant correlation exists between the extent of PPA and glaucomatous damage in the optic nerve head (ONH)[4,6–8] and visual fields.[6,9–12] In addition, several longitudinal studies have reported that PPA seems to be associated with the progression of glaucomatous visual field damage (VFD).[13–17] One study reported that an increase in the extent of PPA paralleled the exacerbation of glaucomatous VFD,[14] and other studies showed the correlation between PPA and the development of glaucoma in eyes with ocular hypertension.[18–21]

In glaucomatous eyes, some differences have been found between the superior and inferior regions of the VFD, ONH morphologic condition, or PPA. For example, as to the VFD, more vulnerability was observed in the superior hemifield in eyes with normal-tension glaucoma (NTG),[22] patients with open-angle glaucoma and diabetes mellitus,[23,24] or patients with NTG with ischemic changes on cerebral magnetic resonance imaging.[25] Early glaucomatous changes are found more often in the inferior region of the ONH,[26] and PPA spreads more widely in the inferior area in healthy or glaucomatous eyes.[10] To our knowledge, however, whether the association among VFD, ONH morphologic condition, and PPA is different between the superior and inferior regions has never been investigated. The purpose of this cross-sectional study was to evaluate VFD, ONH morphologic condition, and PPA in the superior and inferior areas separately and to estimate the correlation of the superior or inferior half areas of PPA with the corresponding hemifield VFD.

0002-9394/06/$32.00
doi:10.1016/j.ajo.2006.01.087

METHODS

ONE HUNDRED NINE CONSECUTIVE PATIENTS WITH NTG who met the inclusion criteria were enrolled in this cross-sectional study between January 2001 and December 2002 at the Department of Ophthalmology, University of Tokyo, Graduate School of Medicine. The study was approved by the Institutional Review Board and adhered to the tenets of the Declaration of Helsinki. Informed consent was obtained from all patients. The inclusion criteria consisted of NTG that had been diagnosed before this study, age ≤60 years, refractive error (spheric equivalent) within ±8 diopters, absence of fundus abnormalities or media opacities except slight cataract, availability of reliable visual field test results (that is, <20% fixation errors, <33% false-positive results, and <33% false-negative results) with the full-threshold or Swedish interactive threshold algorithm (SITA)-standard strategy of the 30 to two program of the Humphrey field analyzer (Carl Zeiss Meditec, Dublin, California, USA), a mean deviation obtained with Humphrey field analyzer better than −25 decibels (dB), the ability to obtain reliable measurements of the Heidelberg Retina Tomograph (HRT; Heidelberg Engineering GmbH, Dossenheim, Germany; that is, a topography standard deviation of ≤30 μm), inclination of the longest meridian of the ONH within 10 degrees of the vertical meridian on the HRT image, and PPA not exceeding the HRT imaging area. If both eyes of a patient met the inclusion criteria, the data from the right eye were used. A diagnosis of NTG was made according to the typical glaucomatous findings in the ONH and corresponding VFD in eyes with consistently normal intraocular pressure levels and the absence of any contributing ocular or systemic disorders. Normal intraocular pressure was defined as that never exceeding 21 mm Hg, including 24-hour fluctuations, without the use of ocular hypotensive medication during the follow-up period.

Visual field and ONH topography were obtained within an interval of ≤three months. The visual fields were tested with the full-threshold or SITA-standard strategy of the 30 to 2 program of the Humphrey field analyzer. The total deviation (TD) values, except the four uppermost edge values that are more vulnerable to the upper lid artifact,[27] were averaged in the superior and inferior hemifields to obtain the superior TD_{mean} and inferior TD_{mean}, respectively.

ONH topography was obtained with the HRT (version 1.11). The HRT parameters that were studied were disk area, cup area, rim area, height variation contour, cup-shape measure, and mean retinal nerve fiber layer thickness. These parameters were first determined for the global disk region. The parameters corresponding to the superior (185 degrees to 5 degrees in a right eye) and inferior (5 degrees to 185 degrees) regions of the ONH, then were determined separately with software provided by the manufacturer.[28]

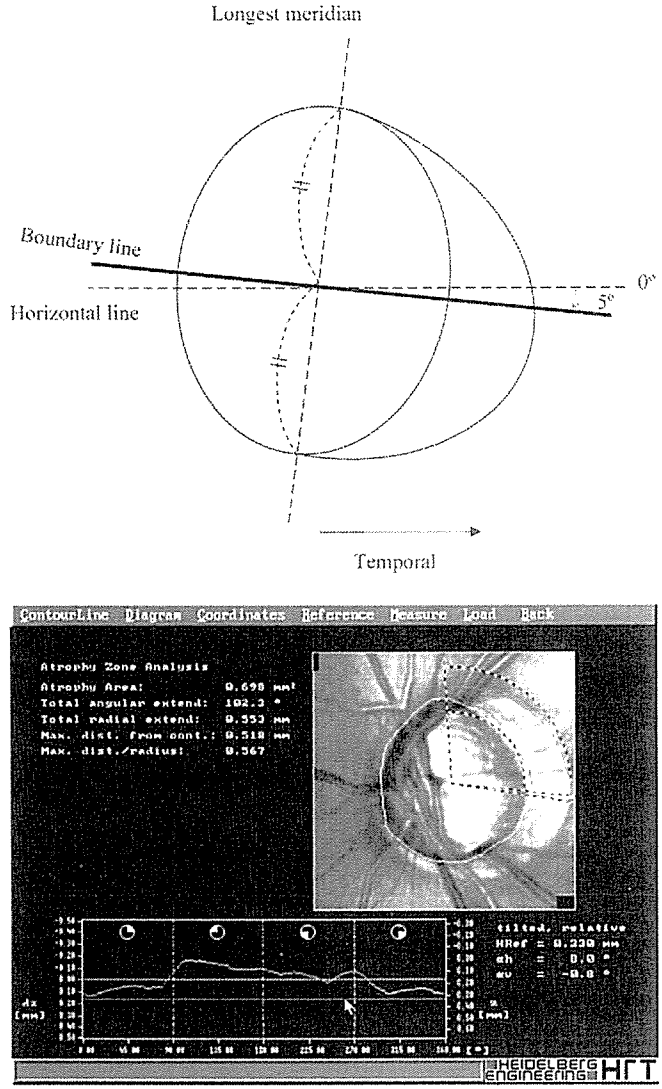

FIGURE 1. Measurement of the superior and inferior areas of parapapillary atrophy.[10] First, the central point of the longest meridian of the disk is determined, and a line is drawn through the central point 5 degrees inferior (temporal side) to the horizontal line (Top). The area of parapapillary atrophy is determined for the superior and inferior half regions, respectively. An example of the measurement of the superior area of parapapillary atrophy in a left eye of a patient with normal-tension glaucoma on a Heidelberg retina tomograph image is shown (Bottom). The superior area of parapapillary atrophy is drawn manually and is shown in blue line on the image. The area of the superior parapapillary atrophy is determined as 0.698 mm^2.

PPA usually is divided into zone α (located peripherally and characterized by irregular hypopigmentation, hyperpigmentation, or both) and zone β (located more centrally with visible large choroidal vessels and visible sclera; Figure 2). It is often difficult to draw the shape of zone α clearly on a fundus photograph or a HRT display, so poorer reproducibility and weaker correlation with VFD has been reported to be a comparison between zone α and zone

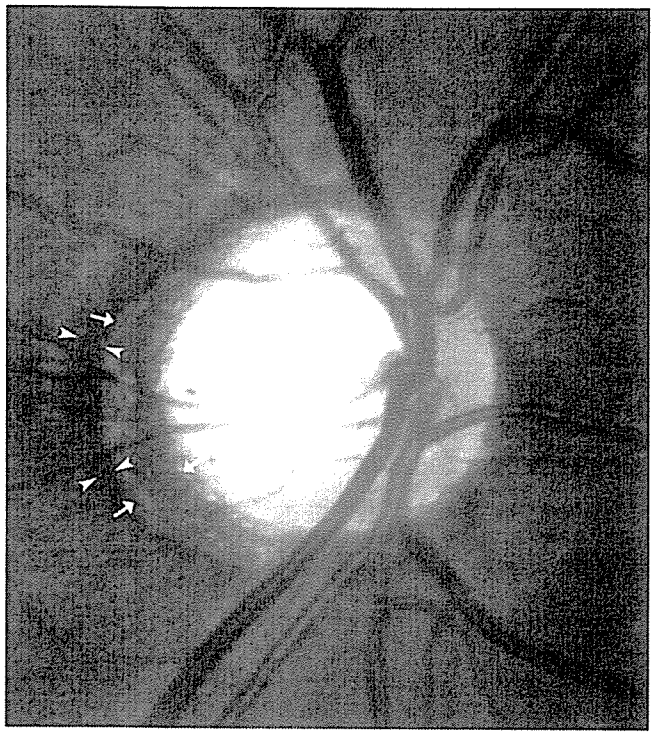

FIGURE 2. An example of glaucomatous optic disk with parapapillary atrophy area of an eye with normal-tension glaucoma. Parapapillary atrophy is divided into "zone α" (white arrow heads), which is located peripherally and characterized by irregular hypopigmentation, hyperpigmentation, or both, and "zone β" (white arrows), which is located more centrally with visible large choroidal vessels and visible sclera.

β.[6,10] Therefore, we measured the area of zone β alone in the current study. The total, superior half, and inferior half areas of zone β were determined on the HRT images as reported previously[10] with the help of color fundus photographs, if necessary (Figure 1). The axial length and refractive error were evaluated with A-scan ultrasonography (AL-2000; Tomey Corporation, Nagoya, Japan) and automated refractometry (ARK-900; Nidek, Aichi, Japan), respectively.

Statistical analyses were carried out with SPSS software for Windows (version 11.01J; SPSS Japan Inc, Tokyo, Japan). The Wilcoxon signed rank test was used to compare the mean values of the superior and inferior regions of the ONH and PPA. Spearman's rank correlation coefficient (Rs) was used to assess the simple correlations between the areas of PPA and age, refraction, axial length, visual field indices, or the HRT parameters. Multiple regression analysis was performed to assess the factors that related to the PPA area in which the dependent variable was the superior or inferior area of PPA; the independent variables were age, axial length, the corresponding disk area obtained with the HRT, and the corresponding VFD indices (superior TD_{mean} or inferior TD_{mean}). Refractive error was not included in the multiple regression model because it was correlated strongly with the axial length (Rs = −0.73).

RESULTS

IN THE 109 EYES FROM 109 PATIENTS WITH NTG, AGE, refractive error, and axial length averaged 48.7 ± 9.2 (mean ± SD) years, −3.41 ± 2.76 diopters, and 25.03 ± 1.41 mm, respectively. The mean deviation, pattern standard deviation, superior TD_{mean}, and inferior TD_{mean} were −6.53 ± 4.74, +9.00 ± 5.04, −8.42 ± 8.51, and −4.81 ± 5.74 dB, respectively. The superior TD_{mean} was significantly lower than the inferior TD_{mean} ($P = .002$).

There were no significant differences in cup area ($P = .37$), rim area ($P = .89$), and cup-shape measure ($P = .39$) between the superior and inferior regions of the ONH, whereas the disk area ($P < .001$), height variation contour ($P = .007$), and mean retinal nerve fiber layer thickness ($P < .001$) were significantly greater in the superior regions than in the inferior regions. The inferior area of PPA was significantly larger than the superior area ($P < .001$; Table 1).

Simple correlation analyses showed significant correlation between the inferior PPA area and the superior hemifield VFD (Rs = −0.32; $P < .001$) but not between the superior PPA area and the inferior hemifield VFD (Rs = 0.05; $P = .6$). Age, refractive error, axial length, and height variation contour were associated significantly with the total, superior, and inferior areas of PPA, respectively ($P < .01$; Table 2).

The multiple regression analyses showed that the superior PPA area was associated significantly with only axial length ($P < .001$) and that the inferior PPA area was associated significantly with the superior hemifield VFD and the axial length ($P < .001$; Table 3).

DISCUSSION

SOME PPA IS THOUGHT TO REPRESENT MISALIGNMENT OF the retinal pigment epithelium, the choroid, and the sclera, which might occur developmentally or might be due to ocular stretching as axial myopia develops.[29] PPA is also thought to result from the age-related changes in the peripapillary retinal pigment epithelium or acquired atrophy of the choroid, retinal pigment epithelium, or both because of ocular diseases that include glaucoma.[30,31] Thus, PPA in glaucomatous eyes might consist of both misalignment because of developmental or myopic factors and pathologic or acquired factors that include glaucoma, although a definitive delineation may be impossible. In the current study, the superior PPA area was correlated significantly with axial length alone, whereas the inferior PPA area was correlated significantly with axial length and the superior hemifield VFD. It suggests that factors that relate

TABLE 1. Heidelberg Retinal Tomography and Parapapillary Atrophy Parameters of the Optic Nerve Head of 109 Eyes With Normal-tension Glaucoma

Parameter	Global	Superior	Inferior	*P* value*
Heidelberg retinal tomography				
Disk area (mm^2)	2.21 ± 0.57	1.12 ± 0.28	1.10 ± 0.30	<.001
Cup area (mm^2)	1.07 ± 0.57	0.57 ± 0.29	0.55 ± 0.31	.37
Rim area (mm^2)	1.14 ± 0.33	0.56 ± 0.19	0.56 ± 0.20	.89
Height variation contour (mm)	0.39 ± 0.14	0.36 ± 0.13	0.34 ± 0.14	.007
Cup-shape measure	−0.088 ± 0.074	−0.054 ± 0.081	−0.064 ± 0.082	.39
Mean retinal nerve fiber layer thickness (mm)	0.225 ± 0.091	0.250 ± 0.099	0.207 ± 0.099	<.001
Parapapillary atrophy				
Area (mm^2)	0.84 ± 0.63	0.37 ± 0.32	0.48 ± 0.38	<.001
Angular extent (degree)	114 ± 60	—	—	—
Radial extent (mm)	0.49 ± 0.31	—	—	—

The data are expressed as the mean ± SD.
*For comparison of mean values of the superior half and inferior regions (Wilcoxon's signed rank test).

TABLE 2. Correlation Coefficients With Parapapillary Atrophy Areas in Simple Correlation Analyses in Patients With Normal-tension Glaucoma

Variable	Total PPA Area	Superior PPA Area	Inferior PPA Area
Age	−0.33 (<.001)	−0.29 (.002)	−0.33 (<.001)
Refractive error	−0.52 (<.001)	−0.46 (<.001)	−0.49 (<.001)
Axial length	0.53 (<.001)	0.50 (<.001)	0.49 (<.001)
Corresponding Heidelberg retinal tomography parameters*			
Disk area	NS (.50)	NS (.75)	NS (.77)
Cup area	NS (.22)	NS (.67)	NS (.71)
Rim area	NS (.12)	NS (.67)	NS (.56)
Height variation contour	0.35 (<.001)	0.43 (<.001)	0.24 (.013)
Cup shape measure	NS (.19)	NS (.22)	NS (.64)
Mean retinal nerve fiber layer thickness	0.26 (.007)	0.29 (.003)	NS (.096)
Visual field indices			
Mean deviation	NS (.07)	—	—
Superior total deviation$_{mean}$	—	—	−0.32 (<.001)
Inferior total deviation$_{mean}$	—	NS (.93)	—

NS = not significant ($P \geq .05$); PPA = parapapillary atrophy.
*The global, inferior, and superior Heidelberg retinal tomography parameters for the comparison with the total, superior, and inferior areas of parapapillary atrophy, respectively. Values indicate Spearman's rank correlation coefficients with the probability values in parentheses.

to the development of glaucoma may be associated dominantly with the inferior area of PPA and that factors that relate to myopia may be associated with both of the superior and inferior areas of PPA.

We estimated the total area of PPA to be 0.84 ± 0.63 mm^2 in the NTG eyes, which was greater than that reported by Park and associates[10] (0.52 ± 0.41 mm^2). As mentioned earlier, the area of PPA should be associated with VFD and the refractive error. Because the mean deviation in the study of Park and associates (−6.00 ± 5.80 dB) was similar to ours (−6.53 ± 4.74 dB), the differences in the refractive errors (−0.30 ± 2.68 vs −3.41 ± 2.76 diopters) between the studies might be responsible for this discrepancy in the area of PPA.

Only weak and nonsignificant correlation (Rs = −0.17; $P = .07$) was found between the total area of PPA and the mean deviation of VFD in the present study. Jonas and Naumann[6] reported a significant correlation between the PPA area and VFD with a correlation coefficient of −0.36 in 582 glaucomatous and 390 normal eyes. Park and associates[10] also reported a correlation coefficient of −0.39 in 105 patients with NTG. The degrees of myopia, which were −0.07 ± 2.18 diopters[6] and −0.30 ± 2.26[10] diopters in those studies, were less than our patients (−3.41 ± 2.76 diopters). The influence of myopia on the extent of PPA[32] might have masked and weakened the correlation between PPA area and mean deviation in this study.

TABLE 3. Multiple Regression Analyses of Factors Relating to Superior or Inferior Areas of Parapapillary Atrophy in Patients With Normal-tension Glaucoma

Parameter	Superior PPA		Inferior PPA	
	Standardized β*	*P* Value	Standardized β*	*P* Value
Age (y)	−.16	.08	−.16	.07
Axial length (mm)	.44	<.001	.40	<.001
Corresponding disk area (mm^2)†	−.006	.94	.03	.70
Superior total deviation$_{mean}$	—	—	−.29	<.001
Inferior total deviation$_{mean}$	.01	.90	—	—

With these regression models, the squared correlation coefficient was 0.25 ($P < .001$) and 0.33 ($P < .001$) for the superior and inferior areas of parapapillary atrophy, respectively.

*Standardized β = Standardized partial regression coefficient.

†Superior or inferior disk area corresponding to the area of parapapillary atrophy, respectively.

PPA = parapapillary atrophy.

The superior hemifield is damaged more often in early-to-moderate open-angle glaucoma[33] or angle-closure glaucoma.[34] The superior area just above the horizontal meridian is more vulnerable, especially in NTG eyes.[22] The inferior hemifield was reportedly more likely to sustain damage in patients with open-angle glaucoma with diabetes mellitus[23,24] or in patients with NTG with ischemic changes on cerebral magnetic resonance imaging.[25] The most frequently occurring visual field defect in nonarteritic anterior ischemic optic neuropathy is an altitudinal defect that involves the inferior hemifield.[35,36] Those studies suggest the presence of different characteristics between the superior and inferior regions of visual field or the ONH regarding the vulnerability to increased intraocular pressure or other challenges. Our results (that a significant correlation with the corresponding VFD was found only for the inferior PPA area but not for the superior PPA area) suggest that PPA itself or the causes of PPA might reflect the differences in vulnerability between the superior and inferior regions of the ONH.

The importance of evaluating PPA in diagnosis and/or follow-up of glaucoma has been recognized widely.[1–21] Because only patients with NTG were included in this study, the influence of intraocular pressure on the development of PPA is hard to determine with these data, and further investigation on patients with open-angle glaucoma with elevated intraocular pressure should be necessary. The results of the current study suggest that the inferior area of PPA may have more clinical importance in association with glaucoma. The differences in correlations with VFD between the superior and inferior areas of PPA may be noteworthy when considering the vulnerability of the ONH in patients with NTG.[30]

REFERENCES

1. Jonas JB, Nguyen XN, Gusek GC, et al. Parapapillary chorioretinal atrophy in normal and glaucoma eyes: I, morphometric data. Invest Ophthalmol Vis Sci 1989;30:908–918.
2. Jonas JB, Budde WM, Lang PJ. Parapapillary atrophy in the chronic open-angle glaucomas. Graefes Arch Clin Exp Ophthalmol 1999;237:793–799.
3. Jonas JB, Bergua A, Schmitz-Valckenberg P, et al. Ranking of optic disc variables for detection of glaucomatous optic nerve damage. Invest Ophthalmol Vis Sci 2000;41:1764–1773.
4. Tezel G, Kass MA, Kolker AE, et al. Comparative optic disk analysis in normal pressure glaucoma, primary open-angle glaucoma, and ocular hypertension. Ophthalmology 1996;103:2105–2113.
5. Park KH, Park SJ, Lee YJ, et al. Ability of peripapillary atrophy parameters to differentiate normal-tension glaucoma from glaucoma-like disk. J Glaucoma 2001;10:95–101.
6. Jonas JB, Naumann GO. Parapapillary chorioretinal atrophy in normal and glaucoma eyes: II, correlations. Invest Ophthalmol Vis Sci 1989;30:919–926.
7. Jonas JB, Fernández MC, Naumann GO. Glaucomatous parapapillary atrophy: occurrence and correlations. Arch Ophthalmol 1992;110:214–222.
8. Hayakawa T, Sugiyama K, Tomita G, et al. Correlation of the peripapillary atrophy area with optic disk cupping and disc hemorrhage. J Glaucoma 1998;7:306–311.
9. Jonas JB, Gusek GC, Fernández MC. Correlation of the blind spot size to the area of the optic disk and parapapillary atrophy. Am J Ophthalmol 1991;111:559–565.
10. Park KH, Tomita G, Liou SY, et al. Correlation between peripapillary atrophy and optic nerve damage in normal-tension glaucoma. Ophthalmology 1996;103:1899–1906.
11. Jonas JB, Gründler AE. Correlation between mean visual field loss and morphometric optic disk variables in the open-angle glaucomas. Am J Ophthalmol 1997;124:488–497.
12. Kono Y, Zangwill L, Sample PA, et al. Relationship between parapapillary atrophy and visual field abnormality in primary open-angle glaucoma. Am J Ophthalmol 1999;127:674–680.
13. Araie M, Sekine M, Suzuki Y, et al. Factors contributing to the progression of visual field damage in eyes with normal-tension glaucoma. Ophthalmology 1994;101:1440–1444.

14. Uchida H, Ugurlu S, Caprioli J. Increasing peripapillary atrophy is associated with progressive glaucoma. Ophthalmology 1998;105:1541–1545.
15. Daugeliene L, Yamamoto T, Kitazawa Y. Risk factors for visual field damage progression in normal-tension glaucoma eyes. Graefes Arch Clin Exp Ophthalmol 1999;237:105–108.
16. Tezel G, Siegmund KD, Trinkaus K, et al. Clinical factors associated with progression of glaucomatous optic disc damage in treated patients. Arch Ophthalmol 2001;119:813–818.
17. Jonas JB, Martus P, Budde WM, et al. Small neuroretinal rim and large parapapillary atrophy as predictive factors for progression of glaucomatous optic neuropathy. Ophthalmology 2002;109:1561–1567.
18. Jonas JB, Martus P, Horn FK, et al. Predictive factors of the optic nerve head for development or progression of glaucomatous visual field loss. Invest Ophthalmol Vis Sci 2004;45:2613–2618.
19. Tezel G, Dorr D, Kolker AE, et al. Concordance of parapapillary chorioretinal atrophy in ocular hypertension with visual field defects that accompany glaucoma development. Ophthalmology 2000;107:1194–1199.
20. Tezel G, Kolker AE, Kass MA, et al. Parapapillary chorioretinal atrophy in patients with ocular hypertension: I, an evaluation as a predictive factor for the development of glaucomatous damage. Arch Ophthalmol 1997;115:1503–1508.
21. Tezel G, Kolker AE, Wax MB, et al. Parapapillary chorioretinal atrophy in patients with ocular hypertension: II, an evaluation of progressive changes. Arch Ophthalmol 1997;115:1509–1514.
22. Araie M, Yamagami J, Suzuki Y. Visual field defects in normal-tension and high-tension glaucoma. Ophthalmology 1993;100:1808–1814.
23. Zeiter JH, Shin DH, Baek NH. Visual field defects in diabetic patients with primary open-angle glaucoma. Am J Ophthalmol 1991;111:581–584.
24. Zeiter JH, Shin DH. Diabetes in primary open-angle glaucoma patients with inferior visual field defects. Graefes Arch Clin Exp Ophthalmol 1994;232:205–210.
25. Suzuki J, Tomidokoro A, Araie M, et al. Visual field damage in normal-tension glaucoma patients with or without ischemic changes in cerebral magnetic resonance imaging. Jpn J Ophthalmol 2004;48:340–344.
26. Kamal DS, Viswanathan AC, Garway-Heath DF, et al. Detection of optic disc change with the Heidelberg retina tomograph before confirmed visual field change in ocular hypertensives converting to early glaucoma. Br J Ophthalmol 1999;83:290–294.
27. Suzuki Y, Araie M, Ohashi Y. Sectorization of the central 30 degrees visual field in glaucoma. Ophthalmology 1993;100:69–75.
28. Wu LL, Suzuki Y, Kunimatsu S, et al. Frequency doubling technology and confocal scanning ophthalmoscopic optic disc analysis in open-angle glaucoma with hemifield defects. J Glaucoma 2001;10:256–260.
29. Fantes FE, Anderson DR. Clinical histologic correlation of human peripapillary anatomy. Ophthalmology 1989;96:20–25.
30. Nevarez J, Rockwood EJ, Anderson DR. The configuration of peripapillary tissue in unilateral glaucoma. Arch Ophthalmol 1988;106:901–903.
31. Rockwood EJ, Anderson DR. Acquired peripapillary changes and progression in glaucoma. Graefes Arch Clin Exp Ophthalmol 1988;226:510–515.
32. Jonas JB, Gusek GC, Naumann GO. Optic disk morphometry in high myopia. Graefes Arch Clin Exp Ophthalmol 1988;226:587–590.
33. Hart WM, Becker B. The onset and evolution of glaucomatous visual field defects. Ophthalmology 1982;89:268–279.
34. Lau LI, Liu CJ, Chou JC, et al. Patterns of visual field defects in chronic angle-closure glaucoma with different disease severity. Ophthalmology 2003;110:1890–1894.
35. Repka MX, Savino PJ, Schatz NJ, et al. Clinical profile and long-term implications of anterior ischemic optic neuropathy. Am J Ophthalmol 1983;96:478–483.
36. Tomsak RL, Remler BF. Anterior ischemic optic neuropathy and increased intraocular pressure. J Clin Neuro-Ophthalmol 1989;9:116–118.